

Controlled synthesis of LiCoPO_4 by a solvo-thermal method at 220°C

S.Brutti^{1,2}, J.Manzi¹, D.Di Lecce³, F.Vitucci², A.Paolone², F.Trequatrin^{2,4}, S.Panero³

¹ Dip.Scienze, Un.Basilicata, V.le dell'Ateneo Lucano 10, 85100-Potenza (Italy)

² Istituto dei Sistemi Complessi (ISC-CNR), V.le dei Taurini, 00185-Roma (Italy)

³ Dip.Chimica, Sapienza Un.Roma, P.le A.Moro 5, 00185-Roma (Italy)

⁴ Dip.Fisica, Sapienza Un.Roma, P.le A.Moro 5, 00185-Roma (Italy)

Abstract

In this letter we report the synthesis at low temperature (220°C) by a solvothermal method of highly crystalline LiCoPO_4 . This material is a candidate for application as high-potential cathode in next-generation Li-ion cells. The here presented synthetic route allows a careful tailoring of the sample morphology and leads to morphologically homogeneous particles platelet-like. The obtained material has been fully characterized by synchrotron radiation X-ray diffraction, vibrational spectroscopy, X-ray photoemission spectroscopy and electron microscopies. The synthesized material has been also characterized in lithium cells to highlight its ability to reversibly cycle lithium.

Keywords: LiCoPO_4 , Li-ion cells.

Introduction

LiCoPO₄ (LCP) is a promising material for application in Li-ion cells as high potential cathode [1, 2]. In fact, it is a possible alternative to the commercial LiCoO₂ cathode, that works at 3.7 V vs Li, as well as to other materials for future high-energy/high-power applications [1]. LiCoPO₄ has a theoretical capacity of 167 mAhg⁻¹ and a working potential of 4.8-4.9 V vs. Li [2]. It belongs to the triphylite lithium orthophosphates: the lattice constants, and also the performances in lithium cells, are strongly related to the synthetic procedure followed in its preparation [2]. Many authors reported possible synthetic routes to obtain LCP particles by solid-state [3], wet chemistry [4], sol-gel [5, 6], hydrothermal [7] and other methods [8]. However, as far as we know, a direct evidence of the formation of crystalline LCP particles without high temperature annealing has never been reported. This limitation is a serious drawback, especially in the case of hydrothermal methods. These routes allow the precipitation of well-formed particles at low temperatures (RT to 300°C) and the need of a high temperature step strongly limit a fine tuning of the crystal morphology.

Here we report the synthesis at low temperature by a solvothermal route of well formed, highly crystalline and pure LCP particles. The synthesis product has been characterized by synchrotron X-ray diffraction (XRD), vibrational spectroscopy (infrared IR and Raman), X-ray photoemission spectroscopy (XPS) and electron microscopy (in scanning and transmission modes, SEM and TEM respectively) in order to highlight the structural, morphological and bonding properties of the synthesized material. As a final point, the LCP material has been casted in composite electrode films and tested in a lithium cell to check its ability to reversibly de-intercalate/intercalate lithium.

Experimental method

The composition of the synthesized material has been determined by inductively coupled plasma-atomic emission spectroscopy (ICP-AES) using a Vista MPX Rad-VARIAN instrument.

1
2
3
4
5
6
7
8
9
10
11
12
13
14
15
16
17
18
19
20
21
22
23
24
The XRD experiment has been carried out at the ELETTRA synchrotron radiation source (MCX
beamline, X-ray wavelength = 1.204 Å). XRD has been recorded in the 12-75° 2θ range with steps
of 0.015° (time/step of 2 sec). Structure refinement has been performed by the Rietveld method
using GSAS [9] starting from the olivine lattice [2] (orthorhombic unit cell with space group n°62
Pnma, Li atoms in 4a (0,0,0), Co in 4c ($x_{TM}, \frac{1}{4}, z_{TM}$), P in 4c ($x_P, \frac{1}{4}, z_P$), O in 4c ($x_O, \frac{1}{4}, z_O$) 4c'
($x_{O'}, \frac{1}{4}, z_{O'}$), and 8d ($x_{O''}, y_{O''}, z_{O''}$)). Few constrains have been adopted, in particular the Li:Co:P
ratios have been fixed to the ICP-AES values, and thus occupancies have not been freely optimized;
also Debye-Waller factors have been kept constant ($B=0.2 \text{ \AA}^2$) for all atoms. In summary the
following parameters have been optimized: (a,b,c) lattice parameters, Caglioti coefficients,
Gaussian-to-Laurenzian coefficients, the atomic positions and the anti-site Li/Co cationic disorder.

25
26
27
28
29
30
31
32
33
34
35
36
37
38
39
40
41
42
The IR spectrum has been recorded at the Soleil Synchrotron Radiation facility (AILES beamline)
on polyethylene pellets containing 1 wt.% of LCP. The Raman spectra has been measured on LCP
pellets by the LabRam HR HORIBA Jobin Yvon spectrophotometer with a He-Ne (632.8 nm) laser
source. Sample morphology has been investigated by SEM using a Phenom-FEI instrument and by
TEM using a FEI Tecnai cryo-TEM. XPS spectra have been recorded by a Leybold LHX1
apparatus with a AlK α radiation [10] and fitted by using Peakfit [11]. Binding energies have been
calibrated on the C1s signal by adding 10 wt.% of graphite to the sample.

43
44
45
46
47
48
49
50
51
52
53
54
55
56
57
58
59
60
61
62
63
64
65
The electrode films have been casted on an aluminium foil by doctor-blading a composite slurry
(80% of LCP, 10% of PVdF-HFP (Kynar Flex 2801), 10% of SuperP carbon in tetrahydrofuran).
The mass loading over the aluminium foil is approximately 3 mg cm⁻². Galvanostatic tests have
been performed in the voltage range 3.5 – 5 V at 0.1C rate (1C = 167 mA g⁻¹) by using a MTI
battery analyser and Swagelok-type cells. The cells have been prepared in Ar-filled glove box with
a lithium metal counter electrode and a commercial electrolyte (LP30, Solvionic).

Results and discussion

LCP has been synthesized by a solvothermal route. Two water solutions, one containing LiOH•H₂O (solution A) and another containing LiH₂PO₄, CoSO₄•7H₂O and sucrose (solution B) have been added in sequence to ethylene glycol (EG) under vigorous stirring (EG:H₂O v/v ratio=2:1). The molar ratios of LiH₂PO₄, CoSO₄•7H₂O, LiOH•H₂O and sucrose have been optimized to the values 1:1:1.75:0.3. The obtained purple suspension has been sealed into a 45 mL Teflon-lined autoclave and heated in oven at 220°C for 15 h. The products have been filtered, washed with H₂O/ethanol and dried in oven. Apparently the use of EG as co-solvent and reaction temperature above 180°C are necessary for the precipitation of crystalline and pure LCP materials. Tentative preparations by the simple hydrothermal route failed even at temperature as high as 240°C for 24h.

The XRD pattern of the synthesized material is shown in the figure 1 together with the IR and Raman spectra.

Figure 1.

The XRD pattern can be fully indexed with the expected olivine prototypal lattice [2]: no additional peaks have been observed, thus suggesting the absence of contaminants. The ICP-AES analysis suggests a Li:Co:P ratio of 1:1:1 thus confirming the LiCoPO₄ stoichiometry. The structural refinement results are summarized in the table 1.

Cell constants are in agreement with literature values [2]: the cell volume is slightly expanded compared to samples annealed at high temperatures (approx. +0.6%) and to single crystals (approx. +1.2%). This evidence indirectly confirms the possible occurrence of anti-site metal disorder (estimated concentration 3.2±0.3%) similarly to the isostructural LiFePO₄ [12].

The IR spectra shows vibrational features similar to the LiFePO₄ lattice [13]: the intramolecular stretchings of the PO₄³⁻ anions are observed at (ν_3) 1178, 1100, 1050 and (ν_1) 970 cm⁻¹ whereas the bending bands (ν_2 , ν_4 and $\nu_2+\nu_4$) are found at 640, 576, 550, 507, 475 and 369 cm⁻¹. Below 300 cm⁻¹

other overlapped bands are observed likely attributed to external modes (libration and translations and Li⁺ cage modes) [13].

Table 1. Summary of the Rietveld Refinement results for the LCP material (Li/Co anti-site defects 3.2±0.3%; assumed full occupancies and B=0.2 Å² for all atoms; convergence parameters R_{wp} =2.4% G.o.f. = 1.09).

Structure	Cell parameters	Atomic positions
Orthorhombic lattice N°62 Pnma space group	a=10.219±0.003 b=5.926±0.002 c=4.707±0.004	Li (0,0,0) Co (0.778,¼,0.521) P (0.595,¼,0.083) O ₁ (0.597,¼,0.761) O ₂ (0.954,¼,0.294) O ₃ (0.166,0.045,0.523)

Similarly to IR also Raman peaks can be assigned following the attributions made for LiFePO₄ [13]. The sharp strong peak at 945 cm⁻¹ is assigned to the A_g mode of the ν₁ (symmetric stretching of the PO₄³⁻ anion) whereas the weak peaks at 989 and 1061 cm⁻¹ to the asymmetric stretching ν₃ of the PO₄³⁻ group. The two double peaks at 589-629 cm⁻¹ and 397-446 cm⁻¹ can be assigned to the ν₄ and ν₂ bending modes of the phosphate anion, respectively. The Raman spectra is in very good agreement with the findings of Marketich and coworkers [14].

The morphology of the synthesized material is very homogeneous as highlighted by SEM and TEM in the figure 2. The LCP material is constituted by sub-micrometrical particles having a platelet shape, with hexagonal/octagonal base and thickness of approximately 50-100 nm.

XPS spectra recorded at the Co 2p, P 2p, O 1s binding energies are shown in the figure 3. The XPS signal of the Co 2p, splitted in the 2p_{3/2} and 2p_{1/2} multiplets separated by 15.5 eV [15], is formed by

1 a triple peak at 783.9, 788.0 and 791.4 eV, in good agreement with the observations reported in refs.
2 [16, 17] for other LCP materials. The presence of multiple peaks is not surprising in the case of
3 cobalt, as well as for many others transition metals (see as an example ref. [18]); the main peak
4 binding energy is comparable with that of CoF_2 (i.e. 783.0 eV) [15] thus confirming a +2 oxidation
5 state for surface Co atoms. The P2p binding energy is located at 133.3 eV (peak split in the 3/2 and
6 $\frac{1}{2}$ doublet separated by 0.86 eV) in agreement with the observation in ref. [17] suggesting a +5
7 oxidation state for phosphorous [15]. The O1s XPS signal is found at 533.3 eV, also in this case in
8 agreement with the observation reported in ref. [16], thus confirming a -2 oxidation state for
9 oxygen.
10

11
12
13
14
15
16
17
18
19
20
21
22
23 The analysis of all the experimental results suggests a successful synthesis at 220°C of LCP with
24 line stoichiometry, high crystallinity, high morphological homogeneity and purity, clean surfaces
25 without the presence of synthesis by-products and contaminants on the surface of the platelet
26 particles.
27

28
29
30
31
32
33 As a final characterization the LCP material has been casted in composite thin film on aluminium
34 foils and tested as cathode material in a lithium cell. The lithium de-intercalation/intercalation curve
35 is shown in the figure 4. The LCP material reversibly cycle lithium ions at approximately 4.8 V vs.
36 Li: the oxidation/reduction steps show two plateaus in agreement with the two consecutive biphasic
37 reaction mechanism discussed by Bramnik [19]. The capacity in the first charge slightly exceed the
38 theoretical capacity (167 mAhg^{-1}) thus suggesting the possible occurrence of electrolyte
39 decomposition at high voltage. On the other hand upon discharge the capacity approaches 100
40 mAhg^{-1} without the need of carbon coatings or doping. In this view the here presented synthetic
41 route allows the preparation of an LCP material with superior performances and large room for
42 improvements.
43
44
45
46
47
48
49
50
51
52
53
54
55
56
57
58
59
60
61
62
63
64
65

Bibliography

- 1
2
3
4 [1] W.Howard, R.Sponitz. *J.Power Sources* 165 (2007) 887-891
5
6 [2] S.Brutti, S.Panero. "Recent advances in the development of LiCoPO₄ as high voltage cathode
7 material for Li-ion batteries," in *Nanotechnology for Sustainable Energy*, Washington, DC,
8 ACS symposium series, American Chemical Society (2013) 67-99.
9
10 [3] K.Amine, H.Yasuda, M.Yamaguchi. *Electrochem.Solid State Lett.* 3 (2000) 178-179.
11
12 [4] C. Delacourt, C.Wurm, P.Reale, M.Mocrette, C.Masquelier. *Solid State Ionics* 173 (2004)
13 113-119.
14
15 [5] H.Ehremberg, N.Bramnik, A.Senyshyn. *Solid State Sci.* 11 (2011) 18-28.
16
17 [6] J.Allen, T.Low, J.Wolfestine. *J.Power Sources* 196 (2011) 8656-8661.
18
19 [7] E.Markevich, R.Sharabi, H.Gottlieb, V.Borgel, K.Fridman, G.Salitra, D.Aurbach, G.Semrau,
20 M.Schmit, N.Schall, C.Brueinig. *Electrochem.Comm.* 15 (2012) 22-25.
21
22 [8] T.Long Doan, I. Taniguchi. *Powder Technol.* 217 (2012) 574-580.
23
24 [9] A. Larson, R.Von Dreele. "General Structure Analysis System (GSAS)," Los Alamos
25 National Laboratory Report LAUR 86 (2000).
26
27 [10] J.Castle, H.Chapman-Kpodo, A.Proctor, A.M.Salvi. *J.Electron Spectrosc.Related*
28 *Phenomena* 106 (2000) 65-80.
29
30 [11] XPS Peakfit 4.1 manual
31 <http://www2.warwick.ac.uk/fac/sci/physics/research/condensedmatt/surface/exp/xps/links/xps>
32 [peak_manual.doc](#)
33
34 [12] S.Kandhasamy, K.Nallathamby, M.Minakshi. *Progress Solid State Chem.*40 (2012) 1-5.
35
36 [13] C.Burba, R.Frech. *J.Electrochem.Soc.* 151 (2004) A1032-A1038.
37
38 [14] E.Markevich, R.Sharabi, O.Haik, V.Borgel, G.Salitra, D.Aurbach, G.Semrau, M.Schmidt,
39 N.Schall, C.Stinner. *J.Power Sources* 196 (2011) 6433-6439.
40
41 [15] NIST X-ray Photoelectron Spectroscopy Database, Version 4.1 (National Institute of
42 Standards and Technology, Gaithersburg, 2012); <http://srdata.nist.gov/xps/>
43
44 [16] L.Tan, Z.Luo, H.Liu, Y.Yu. *J.Alloys Compounds* 502 (2010) 407-410.
45
46 [17] A.Rajalakshmi, V.Nithya, K.Karthikeyan, C.Sanjeeviraja, Y.Lee, R.Kalai Selvan. *J.Sol-Gel*
47 *Sci.Technol.* 65 (2013) 399-410.
48
49
50
51
52
53
54
55
56
57
58
59
60
61
62
63
64
65

[18] M.Biesinger, B.Payne, A.Grosvenor, L.Lau, A.Gerson, R.Smart. *Appl.Surf.Sci.* 257 (2011) 2717-2730.

[19] N.Bramnik, K.Nikolowski, C.Baetz, K.Bramnik, H.Ehrenberg. *Chem.Mater.* 19 (2007) 908-915.

1
2
3
4
5
6
7
8
9
10
11
12
13
14
15
16
17
18
19
20
21
22
23
24
25
26
27
28
29
30
31
32
33
34
35
36
37
38
39
40
41
42
43
44
45
46
47
48
49
50
51
52
53
54
55
56
57
58
59
60
61
62
63
64
65

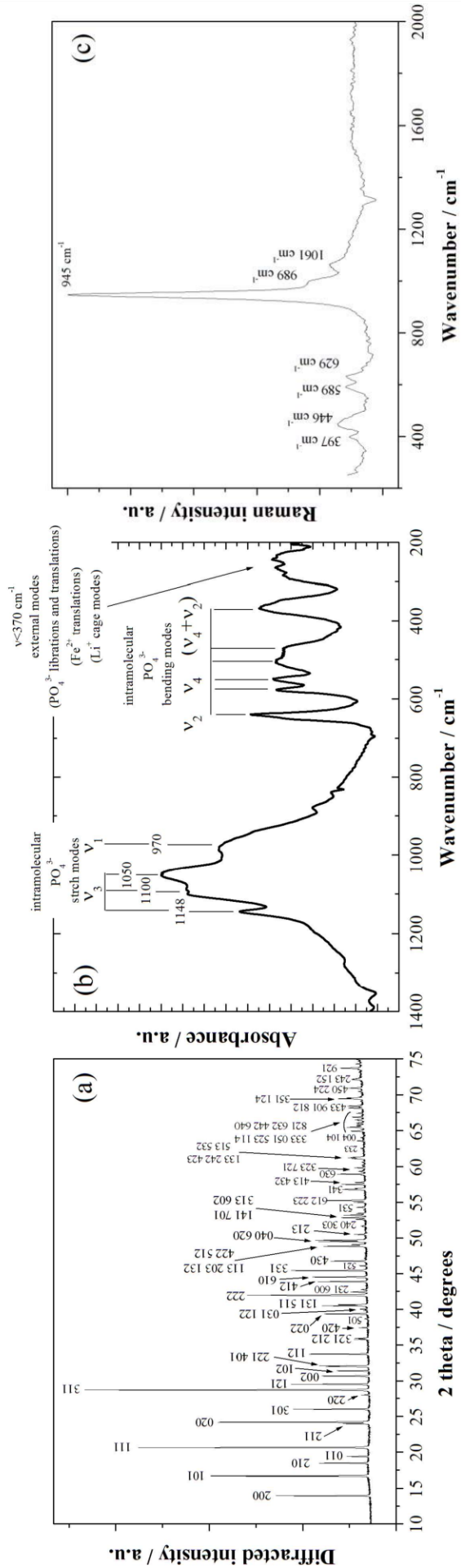


Figure 1. (a) Synchrotron XRD pattern, (b) synchrotron IR and (c) Raman spectra of the as synthesized LCP material

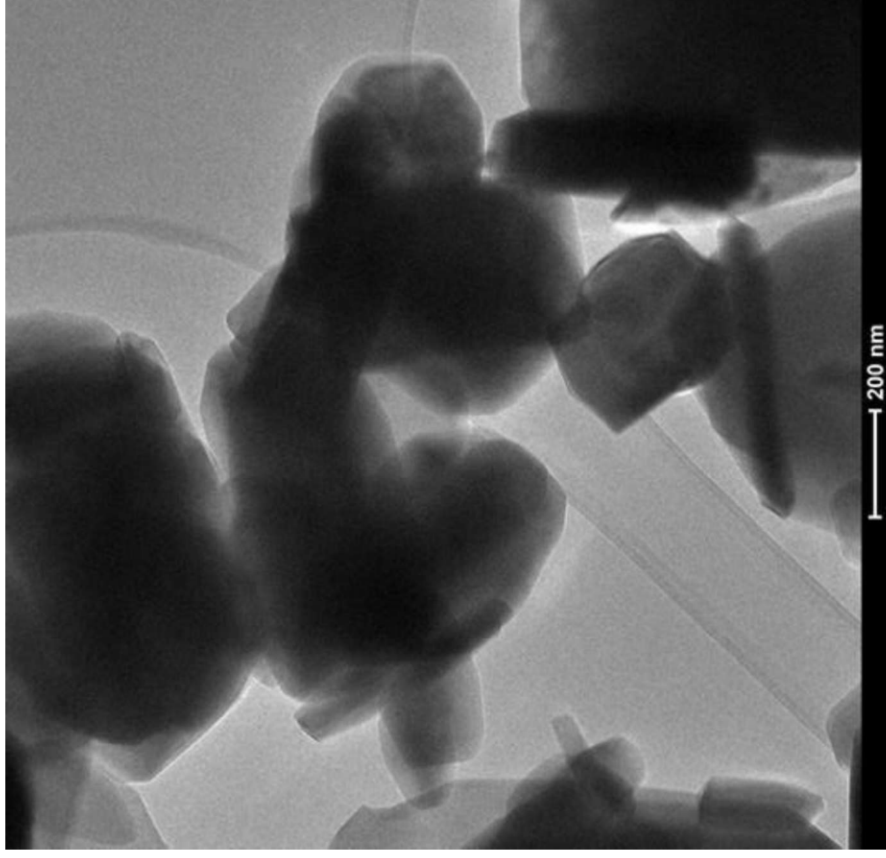
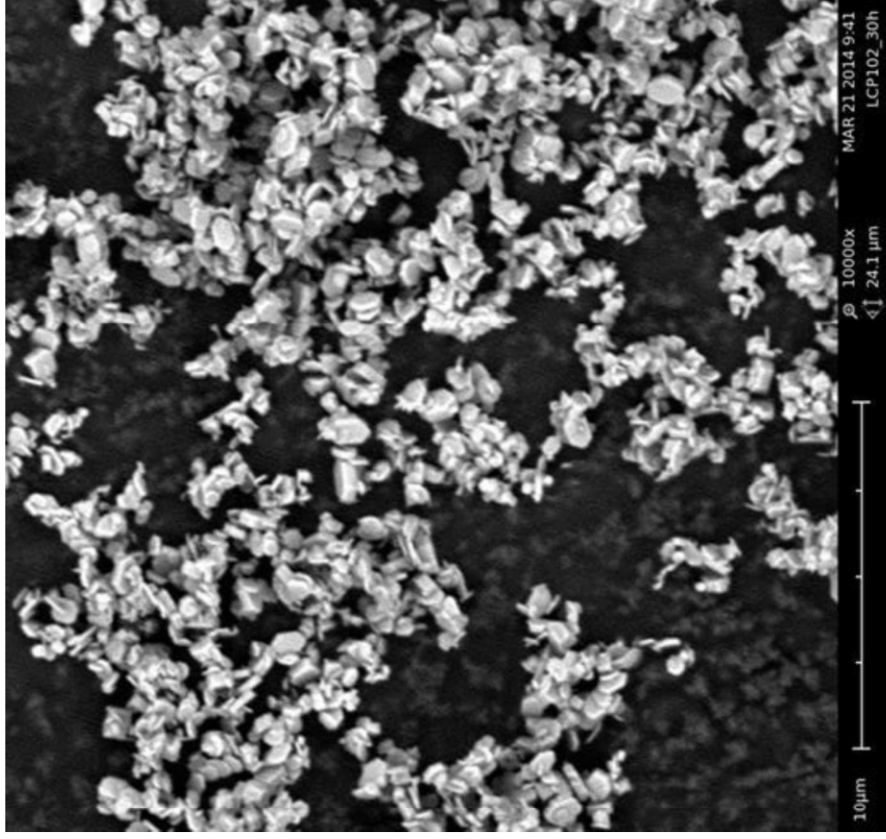


Figure 2. SEM and TEM images of the as-synthesized LCP material

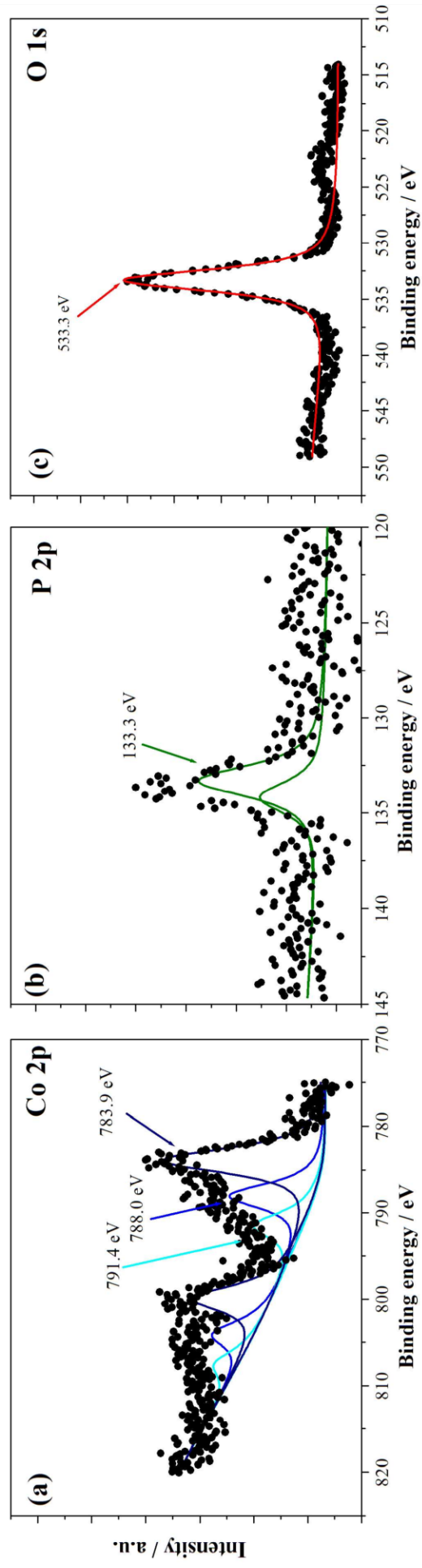


Figure 3. XPS spectra of the as synthesized LCP material: (a) Co 2p, (b) P 2p; (c) O 1s.

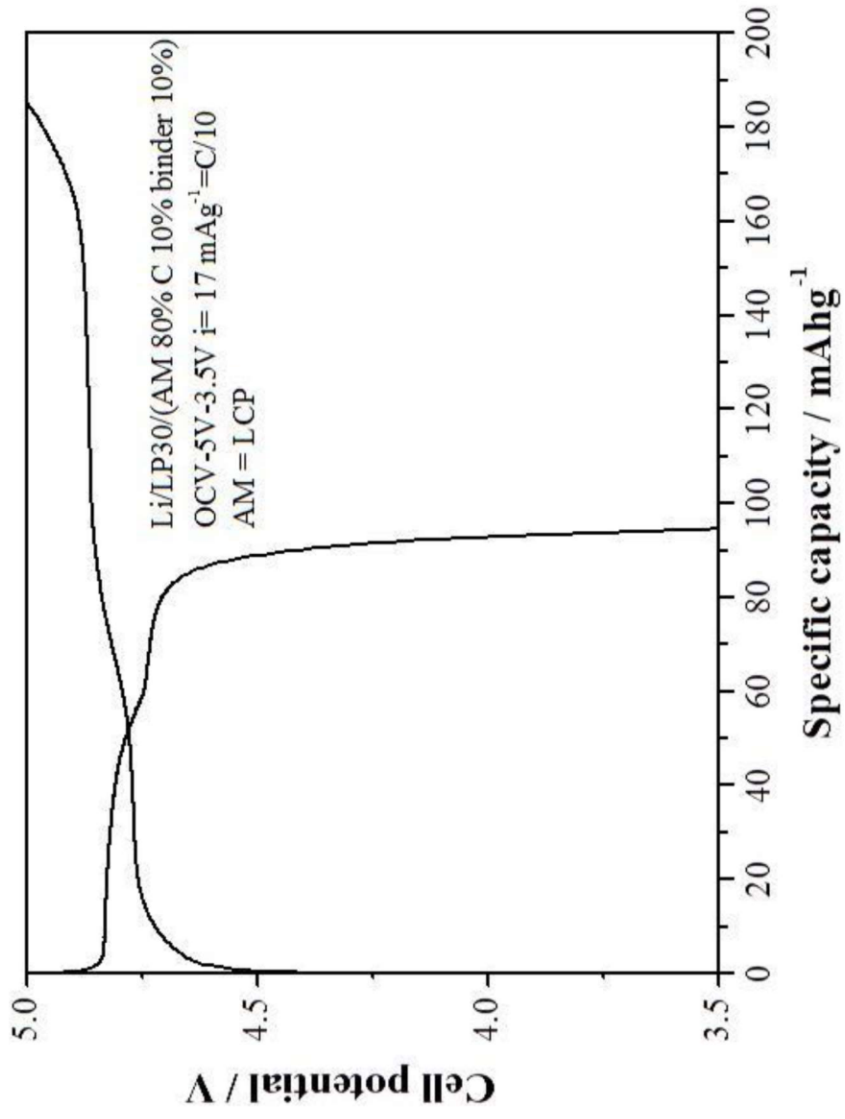


Figure 4. Lithium de-insertion/insertion curve by galvanostatic test in lithium cell